ACADEMIA ROMÂNĂ
Revue Roumaine de Chimie
http://web.icf.ro/rrch/

Rev. Roum. Chim.,
2013, *58*(9-10), 815-821

EFFECT OF ALUMINUM CONTENT FROM MCM-41-TYPE SILICA MATERIALS ON THE IRINOTECAN ADSORPTION AND ITS *IN-VITRO* RELEASE

Laura BAJENARU, Silviu NASTASE, Cristian MATEI* and Daniela BERGER

"Politehnica" University of Bucharest, Faculty of Applied Chemistry and Material Science, 1-7 Polizu street, Bucharest, 011061, Roumania

Received May 13, 2013

Two MCM-41-type aluminosilicate materials were employed as vehicles for the design of irinotecan-based delivery systems. The mesostructured supports were prepared *via* the sol-gel method combined with a hydrothermal treatment using tetraethyl orthosilicate as silicon source and aluminum *sec*-butoxide or sodium aluminate as aluminum precursor. The adsorption of the cytostatic agent on the studied carriers was performed by an impregnation procedure, while its *in-vitro* desorption was carried out in simulated body fluid (SBF – phosphate buffer solution, pH = 7.4). The drug uptakes (around 36%) and retention yields (around 90%) obtained for the aluminosilicates were higher than in the case of MCM-41 silica support. Also, slower delivery kinetics and lower values of the maximum cumulative release for aluminosilicate-type carrier were noticed. These phenomena were ascribed to the acidity induced by the presence of aluminum in the silica framework.

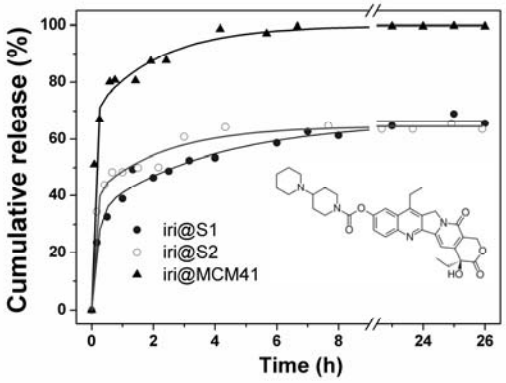

INTRODUCTION

The development of drug delivery systems (DDS) is necessary when conventional administration of a therapeutic agent is not adequate. DDS have some major advantages over the classical pharmacological formulations: controlling the drug release profile in a desired site of the human body, optimizing the dosage, and minimizing the side-effects of the biologically active molecule.[1] In the case of antitumor compounds, the employment of delivery devices with specific site targeted release could significantly reduce the impact of the drug toxicity over the healthy tissues.

The first step in developing a successful DDS represents the right choice of materials used as drug reservoirs.[2] Among these, mesostructured silica can be regarded as efficient carriers due to its suitable features: large specific surface area, high total pore volume, ordered pore array with narrow size distribution. Additionally, the biocompatibility of such materials has been proved to be adequate to the development of new delivery systems.[3] Hence, a large number of biological active molecules with various therapeutic indications were successfully incorporated into silica-based DDS.[4] In most of the studies, the supports was chosen between MCM-41, the pioneer in this field,[5] and SBA-15, both exhibiting hexagonal arrangement of the mesopores.

In order to obtain a hybrid system with an adequate drug release profile, tailored interactions between biological active molecules and the

* Corresponding author: cristi_matei@yahoo.com

mesostructured support should be favored. This can be achieved by functionalization of the pore surface with different organic moieties[4b,h,i,k,l] and/or by the incorporation into the mesostructured framework of different atoms. For example, the introduction of aluminum ions into the silica matrix is accompanied by an increase of the acidity that can influence the drug adsorption and its release.[6,7]

Herein, we report the use of two ordered mesoporous MCM-41 aluminosilicates with different aluminum content as support for drug delivery systems. The selected drug for loading into the mesoporous carriers was irinotecan (Scheme 1), mainly used in the therapy of colon cancer.[8] In recent papers of our group,[9,10] we incorporated irinotecan onto MCM-41-type silica framework and its functionalized derivatives and proposed various kinetic models for its *in-vitro* release behavior. Moreover, we observed an enhanced toxicity of the anticancer agent loaded on the mesostructured supports towards murine embrionary fibroblastic cells.

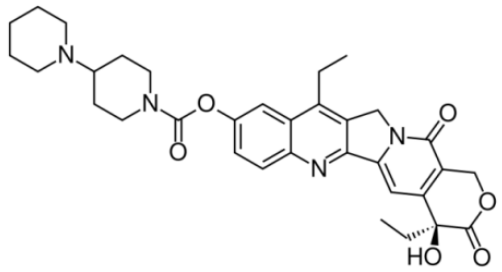

Scheme 1 – Molecular structure of irinotecan.

The aluminosilicate supports were prepared *via* the sol-gel method combined with the hydrothermal treatment using tetraethyl orthosilicate as silicon source and aluminum *sec*-butoxide (**S1** sample) or sodium aluminate (**S2** sample) as aluminum precursor. In order to emphasize the influence of the acidity induced by the presence of aluminum in the silica matrix towards the retention and *in vitro* release of irinotecan molecules, the collected data were compared with our previous study concerning the use of the commercially available MCM-41 support.[9]

RESULTS AND DISCUSSION

Characterization of the mesostructured supports

The detailed description of the supports synthesis was presented elsewhere[11,12] and consequently, only a short recount of the carriers characterization is provided here. The low angle X-ray diffraction patterns (Fig. 1) revealed the presence of the 2D hexagonal pore network, specific to MCM-41-type materials,[3d,13] exhibiting a strong diffraction peak corresponding to {100} Bragg reflection, for all samples. For MCM-41 support, three additionally smaller peaks assigned to {110}, {200}, and {210} reflections are also displayed, characteristic for a long range ordered pore arrays. This feature can be noticed also in the case of the **S1** sample, although the peaks became larger and less intense as result of aluminum incorporation in the silica framework.

All supports employed in this study present type-IV isotherms, reversible in the relative pressure (P/P_0) range of 0-0.45, typical for MCM-41 materials (Fig. 2).[3d,13,14] At $P/P_0 > 0.45$, the isotherms of the supports have hysteresis because of mesopores filling by cappilary condensation of nitrogen. The main textural properties, BET specific surface area calculated from adsorption branch of the isotherm in the relative pressure range of 0.05-0.25, the average pore size determined using Barrett-Joyner-Halenda model (BJH) from desorption branch of isotherm and the total pore volume measured at P/P_0=0.9983, are gathered in Table 1. One can observe the occurrence of pores with the average size situated in the mesopores scale, along with high specific surface area and the total pore volume values.

Table 1

Structural and textural properties of the aluminosilicate-type mesoporous carriers along with the parameters characterizing the processes of irinotecan retention and its *in-vitro* release

Support	Si/Al ratio	S_{BET} (m^2/g)	V_{pore} (cm^3/g)	d_{BJH} (nm)	Irinotecan uptake (%)	Retention yield (%)	Irinotecan maximum cumulative release at 24 h (%)
S1	21	993	0.71	3.34	36.1	89.8	74.0
S2	30	595	0.59	3.45	36.1	89.5	65.6
MCM-41	-	912	1.37	2.76	35	83.7	99.5

The successfully incorporation of aluminum ions into the silica framework was confirmed by X-ray fluorescence technique corroborated with EDX analysis. These measurements demonstrated a relatively uniform composition. The Si/Al molar ratios values, included in Table 1, indicate a higher aluminum content for **S1**, the material prepared using $Al(^{sec}BuO)_3$ as aluminum precursor.

Irinotecan uptake and its in-vitro release

The values of the parameters characterizing the irinotecan uptake and its *in-vitro* release are indicated in Table 1, suggesting a good storage capacity of the aluminosilicate materials for the antitumoral molecules. High irinotecan uptake values (around 36%) and retention yields (around 90%, defined as the ratio between the amounts of irinotecan loaded onto supports and contained in the initial solutions) can be noticed for all three inorganic carriers. Reporting these values to the specific surface area, or to the total pore volume, even higher values were obtained for aluminum containing MCM-41-type supports than for MCM-41 carrier. This enhancement of the drug adsorption could be explained by the synergy between the highly porous nature of the support and the interactions induced by aluminum presence into silica matrix.[12] Besides the hydrogen bonds and host-guest associations, additional electrostatic forces between the positively charged drug molecules (existing in the irinotecan hydrochloride form) and the negatively charged aluminosilicate surface could be possible.

The presence of organic molecules into the mesopores was confirmed by FTIR spectroscopy, wide angle XRD and nitrogen adsorption-desorption isotherms. Wide-angle XRD patterns of hybrid samples proved that the most of cytostatic drug molecules were localized into pores in amorphous state, but a weak tendency of the irinotecan crystallization can be noticed (Fig. 1 – inset). The FTIR spectra were performed before and after the loading procedures. Because the FTIR spectra for the AlMCM-41-type samples and for those of the corresponding hybrid materials are very similar, only the ones involving **S1** support will be discussed here (Fig. 3). A thorough discussion of the infrared absorption spectra belonging to an aluminosilicate-type material was given elsewhere.[12] Typically, several vibration bands, located in the 1200-400 cm^{-1} range revealed the occurrence of AlMCM-41 matrix (1086 cm^{-1}: υ_{as}(Si-O-Si) overlapped with δ(Al-OH); 803 cm^{-1}: υ_{s}(Si-O-Si)) superposed with γ(Al-OH); 957 cm^{-1}: υ(Si-OH); 464 cm^{-1}: δ(Si-O)).[15] Additionally, the large and medium band with maximum at 3438 cm^{-1} is due to the stretching vibration of the associated OH groups, whereas the medium sharp band at 1632 cm^{-1} characterizes the bending deformation of the physiosorbed water, $\delta(H_2O)$. The FTIR spectrum of the hybrid system, iri@S1, (Fig 3b) displays several absorption bands distinctive from the **S1** sample used as support. Two characteristic absorption bands located at 2926 cm^{-1} and 2855 cm^{-1} were ascribed to the asymmetric and symmetric stretching vibrations of the CH_2 groups that belong to the irinotecan molecules (Fig. 3d). The vibration bands situated in the 1600-1750 cm^{-1} range are due to the C=O stretching vibration modes of the irinotecan molecules.[16] The specific vibration modes of the AlMCM-type support were well preserved in the hybrid sample. The irinotecan adsoption into the mesopores of the supports was also proved by type-II N_2 adsoption-desoption isotherms of hybrids, typical for nonporous materials, illustrated for iri@MCM-41 in Fig. 2. The specific surface area and total pore volume values for hybrid samples were in the range of 51-68 m^2/g and 0.07-0.1 cm^3/g, respectively. The scanning electron microscopy (SEM) investigation revealed no significant change in the morphology of hybrid samples (Fig. 4A) in comparison with the corresponding pristine supports (Fig. 4B).

Irinotecan *in-vitro* delivery experiments were carried out at 37 °C under magnetic stirring (120 rpm). At certain time intervals, portions of the fluid were withdrawn and analyzed by UV-Vis spectroscopy. The delivery profiles are displayed in Fig. 5 and are presented as a plot of the cumulative release *versus* time. According to Vallet-Regi *et al*,[3a] these patterns belong to the *a*-type delivery profile, specific to the un-functionalized carriers. These consist in a "burst" effect (a fast desorption of a considerable amount of the drug within the first hours of the experiment) followed by a slow release. Compared with MCM-41 based hybrid (Fig. 5c), whose behavior was described elsewhere,[9] the delivery of irinotecan loaded on aluminosilicate-type carriers (Fig. 5a and b) was slower. This trend could be explained by the presence of Lewis acidic sites responsible for the supplementary interactions occurred between the drug molecules and the carriers. Hence, after 8 hours, the cumulative

release from the hybrid based on the carrier with higher aluminum content (iri@S1) was lower (61.3%) than that of iri@S2 hybrid (63.6%), with lower aluminum content. The pronounced interactions between aluminosilicate-type carrier and irinotecan molecules caused lower cumulative release values in comparison with silica MCM-41 type support, the maximum cumulative release values being 74% (iri@S1) and 65.6% (iri@S2), respectively, as compared with almost 100% for iri@MCM-41. The presence of residual drug molecules in the hybrids isolated after the delivery experiments was proved by FTIR spectra, which preserved vibration bands, although less intense, specific to the drug molecules (Fig. 3c).

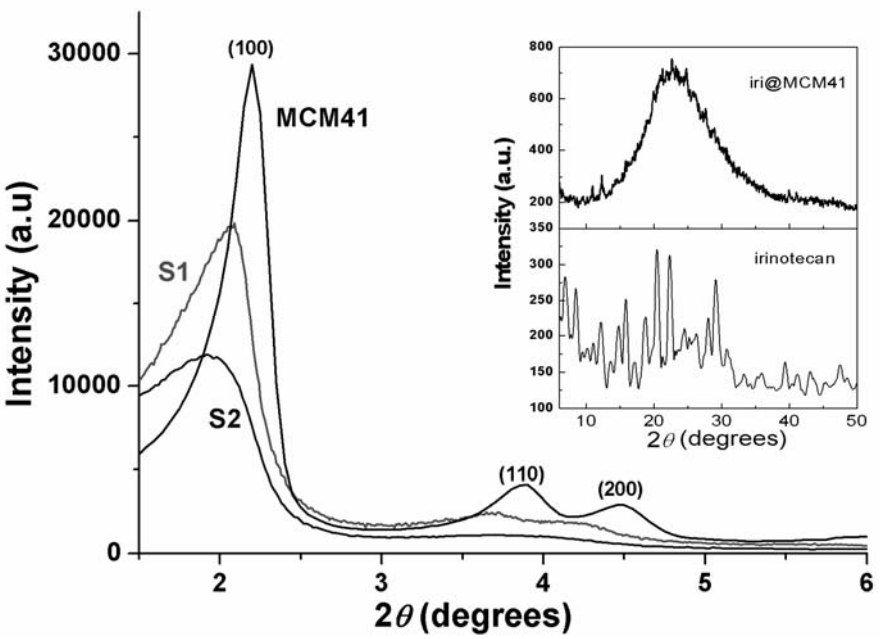

Fig. 1 – Small-angle XRD patterns of the MCM-41-type silica and aluminosilicate supports. Inset-wide-angle XRD of iri@MCM-41 (up) and irinotecan hydrochloride (bottom).

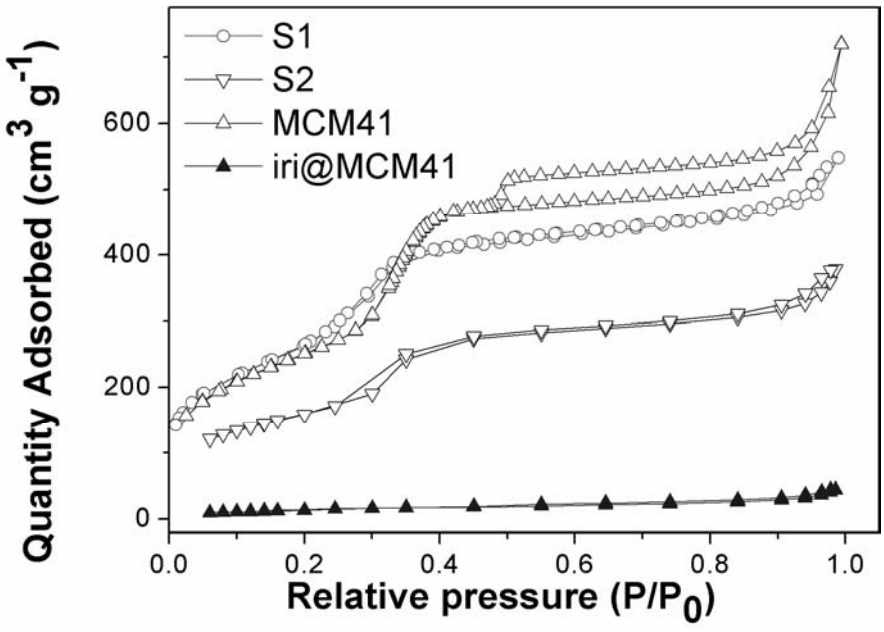

Fig. 2 – N_2 adsorption/desorption isotherms of MCM-41-type supports and iri@MCM-41 hybrid sample.

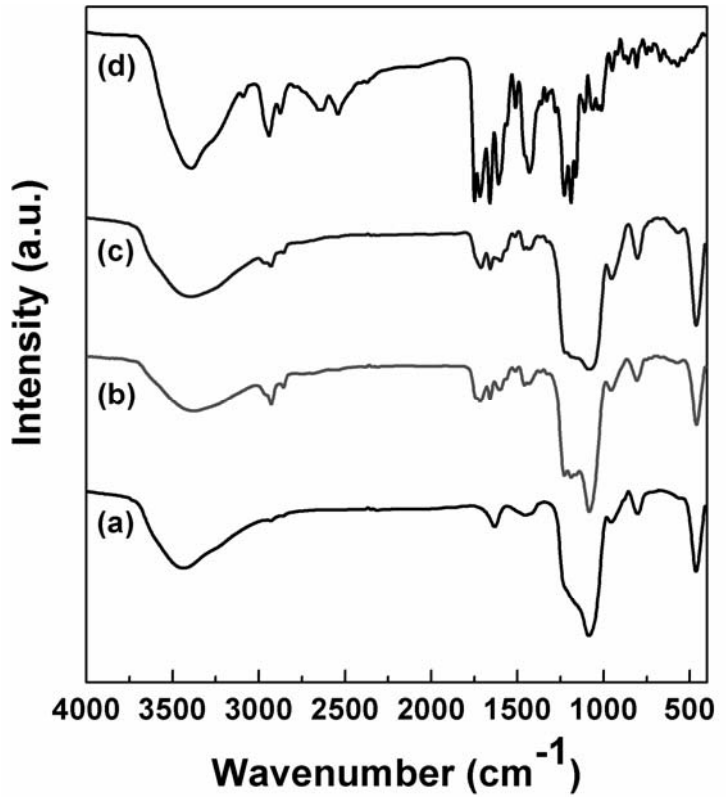

Fig. 3 – FTIR spectra of S1 support (a), iri@S1 hybrid (b), iri@S1f,
the hybrid isolated after the delivery experiment (c), and irinotecan hydrochloride (d).

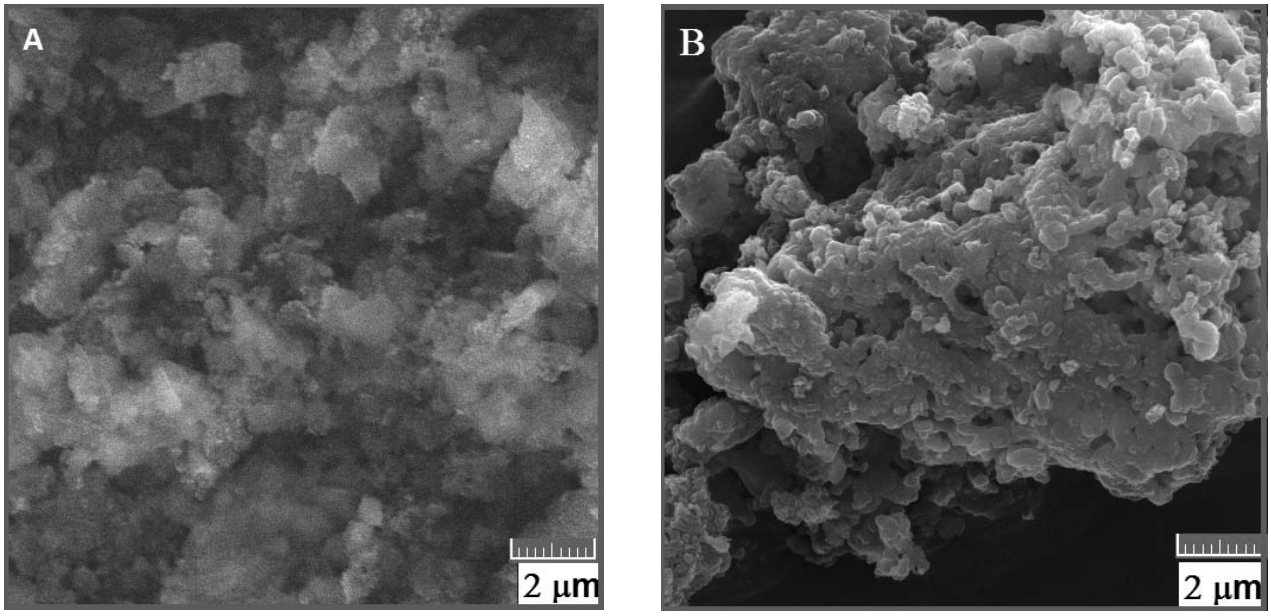

Fig. 4 – SEM micrographs of iri@MCM-41 hybrid sample (A) and MCM-41 support (B).

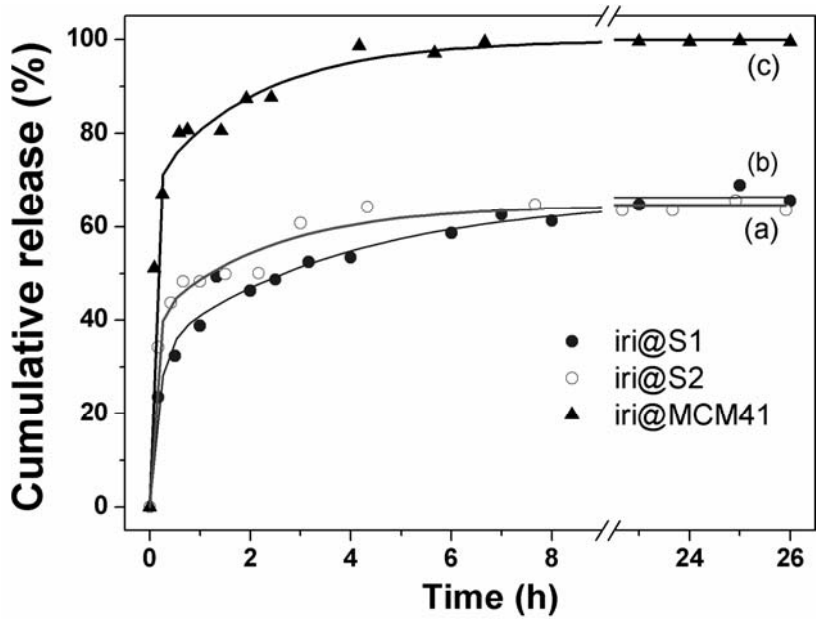

Fig. 5 – Irinotecan *in-vitro* delivery profiles of hybrid samples: iri@S1 (a), iri@S2 (b), iri@MCM-41 (c).

EXPERIMENTAL

Reagents

All the chemicals, tetraethylorthosilicate (TEOS, Fluka 99,0%), sodium aluminate ($NaAlO_2$, Sigma Aldrich), aluminum *sec*-butoxide ($Al(O^{sec}Bu)_3$, Sigma), 1-hexadecyltrimethyl ammonium bromide (CTAB, Merck), MCM-41 (Aldrich), ammonia solution 25% (Scharlau), potassium dihydrogen phosphate (Merck), sodium hydroxide (Sigma-Aldrich), and irinotecan hydrochloride (Sigma) were used as received without further purification.

Synthesis of the supports

AlMCM-41-type materials were synthesized as previously described.[11] Briefly, aluminum *sec*-butoxide (for **S1** sample) and sodium aluminate (for **S2** sample), respectively have been used as aluminum source. A mixture of TEOS and aluminum precursor was slowly added to a solution prepared by the dissolution of the surfactant in deionized water and 25% (wt) aqueous ammonia solution. After the hydrothermal treatment of the resulted white suspension, a calcination step at 550 °C/5h of the isolated powders was performed. To give a reliable correlation between the acidity of the mesostructured samples and the influence of various structural and textural features of the mesoporous supports towards the retention and *in-vitro* release of irinotecan molecules, a commercially available support MCM-41 was also employed.

Irinotecan loading and its in-vitro release

The uptake of the cytostatic agent on the AlMCM-41-type supports and its *in-vitro* delivery were carried out using procedures similar to those reported in our recent paper dealing with the irinotecan loading onto MCM-41 sample and its functionalized derivatives.[9] The biologic active molecule content was monitored by UV-Vis spectroscopy, by measuring the solution absorbance at λ = 255 nm. Previously, the calibration curve was obtained by a linear regression, fitting the experimental data with high correlation coefficient. Typically, irinotecan adsorption was achieved following an impregnation procedure from drug aqueous solution, the resulted hybrid materials being thereafter denoted iri@S1 and iri@S2. The drug delivery experiments were performed by immersing the irinotecan–based hybrids in simulated body fluid (SBF, phosphate buffer solution, pH=7.4).

Materials characterization

Both carrier-type materials and the corresponding hybrid systems were characterized by several techniques. The infrared spectra (in KBr pellets) were collected on a Bruker Tensor 27 spectrophotometer in the 4000-400 cm^{-1} range. The N_2 adsorption/desorption isotherms were measured at 77 K using a Quantachrome Autosorb iQ porosimeter. The small- and wide-angle XRD analyses were performed on a Rigaku MiniFlex II diffractometer with CuKα X-ray radiation (λ=1.5406 Å). The SEM investigation was performed on Tescan Vega III microscope. The Si/Al molar ratios were determined by X-ray fluorescence technique on a Rigaku Sequential X-ray fluorescence spectrometer (ZSX Primus II), corroborated with data from energy dispersive X-ray (EDX) analysis carried out on SEM. The UV-Vis spectra were recorded on Ocean Optics USB 4000 equipment.

CONCLUSIONS

MCM-41-type aluminosilicate materials were employed as support for the design of irinotecan delivery systems. The drug was successfully entrapped into the pores of the mesostructured matrices. The irinotecan uptake values in the resulted hybrid samples and the retention yields were higher than those founded in the case of MCM-41 silica matrix. The higher values of the parameters characterizing the irinotecan adsorption experiments were related to the acidity of the

aluminosilicate carriers, which induced stronger interactions between the biologically active molecules and support. The presence of the aluminum atoms also influenced the profile of the *in-vitro* delivery of irinotecan. A slower desorption, along with a decrease of the maximum cumulative release of the drug was observed for hybrids with high aluminum content. The values of the drug uptake and the shape of the delivery profile suggested that these inorganic matrices are good candidates for elaborating irinotecan-based delivery systems.

Acknowledgements: The financial supports of the European Commission through European Regional Development Fund and of the Roumanian state budget, project POSCCE-O2.1.2-2009-2, ID 691, "New mesoporous aluminosilicate materials for controlled release of biologically-active substances" and Roumanian project PCCA no 131/2012 are gratefully acknowledged.

REFERENCES

1. A.S. Hoffman, *J. Control. Release*, **2008**, *132*, 153-163.
2. See, for example: (a) G.A. Husseini and W.G. Pitt, *Adv. Drug Del. Rev.*, **2008**, *60*, 1137-1152; (b) L. Bromberg, *J. Control. Release*, **2008**, *128*, 99-112; (c) D. Schmaljohann, *Adv. Drug Del. Rev.*, **2006**, *58*, 1655-1670; (d) S.V. Vinogradov, T.K. Bronich and A.V. Kabanov, *Adv. Drug Del. Rev.*, **2002**, *54*, 135-147; (e) C. Boyer and J.A. Zasadzinski, *ACS Nano*, **2007**, *1*, 176-182; (f) R.R. Sawant and V.P. Torchilin, *Soft Mater.*, **2010**, *6*, 4026-4044; (g) S. Svenson and D.A. Tomalia, *Adv. Drug Del. Rev.*, **2005**, *57*, 2106-2129.
3. Several excellent reviews on mesoporous silica materials and/or their employment as drug-delivery systems have been published: (a) M. Vallet-Regi, F. Balas and D. Arcos, *Angew. Chem. Int. Ed.*, **2007**, *46*, 7548-7558; (b) F. Hoffmann, M. Cornelius, J. Morell and M. Froba, *Angew. Chem. Int. Ed*., **2006**, *45*, 3216-3151; (c) S.B. Wang, *Micropor. Mesopor. Mater.*, **2009**, *117*, 1-9; (d) Y. Wan and D.Y. Zhao, *Chem. Rev.*, **2007**, *107*, 2821-2860; (d) J.Y. Ying, C.P. Mehnert and M.S. Wong, *Angew. Chem. Int. Ed*., **1999**, *38*, 56-77; (e) M. Hartmann, *Chem. Mater.*, **2005**, *17*, 4577-4593.
4. See, for example: (a) J. Andersson, J. Rosenholm, S. Areva and M. Linden, *Chem. Mater.*, **2004**, *16*, 4160-4167; (b) S.W. Song, K. Hidajat and S. Kawi, *Langmuir*, **2005**, *21*, 9568-9575; (c) P. Horcajada, A. Ramila, J. Perez-Pariente and M. Vallet-Regi, *Micropor. Mesopor. Mater.*, **2004**, *68*,105-109; (d) A.L. Doadrio, E.M.B. Sousa, J.C. Doadrio, J.Perez-Pariente, I. Izquierdo-Barba and M. Vallet-Regi, *J. Control. Release*, **2004**, *97*, 125-132; (e) M. Vallet-Regi, J.C. Doadrio, A.L. Doadrio, I. Izquierdo-Barba and J. Perez-Pariente, *Solid State Ion.*, **2004**, *172*, 435-439; (f) Z.M. Tao, Y.W. Xie, J. Goodisman and T. Asefa, *Langmuir*, **2010**, *26*, 8914-8924; (g) Q.J. He, J.L. Shi, F. Chen, M. Zhu and L.X. Zhang, *Biomaterials*, **2010**, *31*, 3335-3346; (h) F. Qu, G. Zhu, S. Huang, S. Li and S. Qiu, *ChemPhysChem*, **2006**, *7*, 400-406; (i) F. Sevimli and A. Yilmaz, *Micropor. Mesopor. Mater.*, **2012**, *158*, 281-291; (j) Y. Chen, H.R. Chen, M. Ma, F. Chen, L.M. Guo, L.X. Zhang and J.L. Shi, *J. Mater. Chem.*, **2011**, *21*, 5290-5298; (k) R.F. Popovici, E.M. Seftel, G.D. Mihai, E. Popovici and V.A. Voicu, *J. Pharm. Sci.*, **2011**, *100*, 704-714; (l) J.C. Doadrio, E.M.B. Sousa, I. Izquierdo-Barba, A.L. Doadrio, J. Perez-Pariente and M. Vallet-Regi, *J. Mater. Chem.*, **2006**, *16*, 462-466.
5. M. Vallet-Regi, A. Ramila, R.P. del Real and J. Perez-Pariente, *Chem. Mater.*, **2001**, *13*, 308-311.
6. L. Ji, A. Katiyar, N.G. Pinto, M. Jaroniec and P.G. Smirniotis, *Micropor. Mesopor. Mater.*, **2004**, *75*, 221-229.
7. G. Cavallaro, P. Pierro, F.S. Palumbo, F. Testa, L. Pasqua and R. Aiello, *Drug Deliv.*, **2004**, *11*, 41-46.
8. V. Pavillard, C. Agostini, S. Richard, V. Charasson, D. Montaudon and J. Robert, *Cancer Chemother. Pharmacol.*, **2002**, *49*, 329-335.
9. G. Maria, D. Berger, S. Nastase and I. Luta, *Micropor. Mesopor. Mater.*, **2012**, *149*, 25-35.
10. S. Nastase, L. Bajenaru, D. Berger, C. Matei, M.G. Moisescu, T. Savopol and D. Constantin, *Cent. Eur. J. Chem.*,DOI: 10.2478/s11532-014-0501-y .
11. L. Bajenaru, S. Nastase, C. Matei and D. Berger, *U. Politeh. Buch. Ser. B*, **2011**, *73*, 45-50.
12. S. Nastase, L. Bajenaru, C. Matei and D. Berger, *Micropor. Mesopor. Mater.*, **2013**, *182*, 32-39.
13. Q. Huo, D.I. Margolese and G.D. Stucky, *Chem. Mater.*, **1996**, *8*, 1147-1160.
14. V. Meynen, P. Cool and E.F. Vansant, *Micropor. Mesopor. Mater.*, **2009**, *125*, 170-223.
15. See, for example: (a) P.P. Yang, Z.W. Quan, L.L. Lu, S.S. Huang and J. Lin, *Biomaterials*, **2008**, *29*, 692-702; (b) Y. Li and B. Yan, *Nanoscale Res. Lett.*, **2010**, *5*, 701-708; (c) L.S. Fu, H.J. Zhang and P. Boutinaud, *J. Mater. Sci. Technol.*, **2001**, *17*, 293-298; (d) D. Berger, G.A. Traistaru and C. Matei, *Cent. Eur. J. Chem*., **2012**, *10*, 1688-1695; (e) P. Colomban, *J. Mater. Sci. Lett.*, **1998**, *7*, 1324-1326.
16. G. Socrates, "Infrared and Raman characteristic group frequencies", 3rd edition Chichester, John Wiley and Sons, 2001.